Electronic properties and transformation kinetics of two prominent metastable defects introduced in GaAs during sputter deposition of Au Schottky contacts

F. Taghizadeh, P.J. Janse van Rensburg, K. Ostvar, W.E. Meyer and F.D. Auret

Department of Physics, University of Pretoria, Private Bag X20, Hatfield, 0028, Pretoria, South Africa

*Corresponding author. Email: f.taghizadeh@tuks.co.za

Abstract

Au Schottky barrier contacts (SBDs) were DC sputter deposited on Si doped n-type GaAs at a power of 150 W. Deep-level transient spectroscopy (DLTS) and Laplace DLTS were used to characterize the sputter-induced defects near the surface of the GaAs. In this study, *I-V* and *C-V* measurements showed that the sputter deposited diodes had a significantly lower barrier height and a higher free carrier density. Using DLTS, it was found that this sample contained seven defects – three of them were metastable while one of the others was highly dopant dependent. The energy levels of these defects are E_c – 0.046 eV, E_c – 0.22 eV, E_c – 0.30 eV, E_c – 0.55 eV, E_c – 0.56 eV, E_c – 0.83 eV and E_c – 0.84 eV. The EL2 defect was not observed in the sputtered samples, but one of the sputter-induced defects emitted in the same range as the EL2, however, it had two components and their DLTS signatures (E_c – 0.83 eV and E_c – 0.84 eV) differed significantly from that of the EL2. By applying different bias conditions (−2 V and zero V) for annealing procedures, the metastable defects (E_c – 0.30 eV and E_c – 0.56 eV) were transformed into each other. The pre-factor obtained from transformation rate of E_c – 0.56 eV → E_c – 0.30 eV under reverse bias was 3×10^{15} s^{-1} which is related to free carrier emission.

Keywords: Sputter-deposition induced defects in GaAs; Laplace deep-level transient spectroscopy; Metastability; Transformation kinetics; Near-surface damage

1. Introduction

Schottky barrier diodes (SBDs) play a significant role in very large-scale integration technology [1]. Sputter deposition is one of the methods to fabricate both low and high-barrier SBDs The advantages of sputter deposition are: ability to deposit metals with high melting point, stoichiometric deposition of compounds, high deposition rate and better adhesion than resistive deposition [2,3]. However, the energetic particles involved in this process introduce surface and sub-surface disorder, and these unwanted disorders affect the rectification characteristics of Schottky diodes [2]. The surface and sub-surface disorder introduce defects that have both discrete levels in the semiconductor band gap as well as continuous energy levels [4]. The barrier height of the sputter deposited metal contacts on n-type GaAs are lower than similar resistively-deposited contacts and higher for p-type GaAs [5]. Recently, deep level transient spectroscopy (DLTS) has been used to investigate the defects introduced in epitaxially grown Si-doped and bulk-grown GaAs [3,5,6,7].

Laplace DLTS is a high resolution technique capable of resolving defects with closely spaced emission rates in order to characterize them. In this study, we used high resolution Laplace DLTS, introduced by Dobaczewski et al. in 2004 [8], to investigate the electrical properties in the 20–405 K temperature range of defects introduced during sputter deposition of Au on Si-doped n-type gallium arsenide (GaAs).

2. Experimental procedure

The *n*-GaAs used in this study was grown by metalorganic vapour phase epitaxy (MOVPE) on n^+ GaAs substrates. These samples were doped with Si to 1.0×10^{15} cm^{-3} and 1.0×10^{16} cm^{-3}, respectively. First, the samples were degreased and chemically etched. Thereafter Ni/AuGe/Ni ohmic contacts with thicknesses of 100/1450/300 Å

were fabricated on the back surface, then they were annealed in Ar at 450 °C for 2 min to form the ohmic contact.

After ohmic contact fabrication, samples were cleaned and etched again, and mounted immediately inside the vacuum chamber for the sputter deposition of the Schottky contacts. Circular Au Schottky contacts were sputter deposited through a metal contact mask onto the GaAs layers. The depositions were carried out at a DC power of 150 W at an Ar pressure of 8×10^{-2} mbar with a DC bias of 580 V for 5 min.

For the control sample the cleaning and ohmic contact deposition procedures were the same as for the sputtered samples. After the second cleaning procedure the sample was quickly mounted in the same deposition chamber which was used for ohmic contact fabrication, and 0.6 mm diameter Au Schottky contacts were deposited (1000 Å) on the epitaxially grown surface of the samples through a metal contact mask.

The influence of these sputter-induced defects on the diode properties was assessed by current-voltage (*I-V*) and capacitance-voltage (*C-V*) measurements. The *I-V*/*C-V* measurements were performed at 25 °C, meanwhile the bias was applied by an HP 4140 B pA meter/Voltage source and a HP 4192 LF Impedance analyser, with the voltage monitored with a HP 34401A multimeter. All the control and sputtered samples were measured under the same conditions. The electrical properties of the sputter-induced defects in GaAs were characterized by DLTS and Laplace DLTS in the 20–405 K temperature range. DLTS temperature was measured using a platinum resistance thermometer and bias was applied by a dedicated Laplace DLTS card, monitored by an oscilloscope.

3. Results and discussion

As shown in Fig. 1, the *I-V* characteristics of the control samples were close to ideal, with an ideality factor of 1.02, indicating that thermionic emission was the dominant current transport mechanism. Both the sputtered contacts showed significantly worse *I-V* characteristics, with a higher ideality factor and lowering in barrier height. See Table 1 for details. Despite some deviation from ideality, the ideality factor remained close to one and the reverse leakage current did not increase significantly above the saturation current, indicating that thermionic emission was still the dominant current transport mechanism in the sputtered diodes. The lower doped material showed a higher reverse leakage current, probably due to more carrier generation by the defects in the wider depletion region. In both cases, the sputtered contacts had a higher series resistance than the those on the control samples.

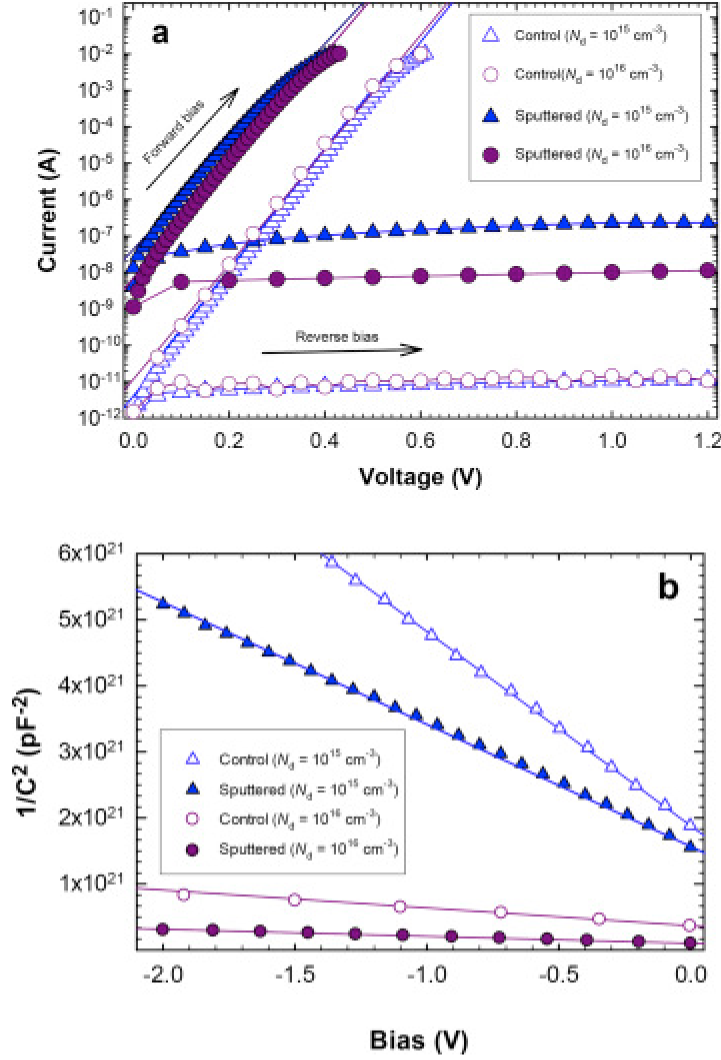

Fig. 1. Demonstrates the change in (a) I-V and (b) C-V plots as a result of sputter deposition of Schottky contacts on 1.0×10^{15} cm^{-3} and 1.0×10^{16} cm^{-3} samples.

Table 1
Diode parameters of n-type GaAs of control and sputter samples (1.0×10^{15} cm^{-3} and 1.0×10^{16} cm^{-3}).

Sample		n	φ_{IV} (eV)	φ_{CV} (eV)	$R_s (\Omega)$	carrier concentration (cm^{-3})
1.0×10^{15} cm^{-3}	control	1.02	0.96	0.97	3.8	1.1×10^{15}
	sputtered	1.15	0.63	0.74	10	3.5×10^{15}
1.0×10^{16} cm^{-3}	control	1.02	0.87	1.72	3.4	1.2×10^{16}
	sputtered	1.11	0.65	1.05	4.8	1.6×10^{16}

The *C-V* characteristics (plotted as $1/C^2$ vs V in Fig. 1) showed constant carrier concentration profiles for the control samples, while the sputtered samples showed a significant increase in carrier concentration and, similar to the *I-V* characteristics, a decrease in barrier height. The C-V barrier heights were higher than the *I-V* barrier heights, indicating that there might have been some barrier height inhomogeneities. The slight deviations from linearity in the *C-V* characteristics indicates a minor variation in the carrier density with depth. It is clear that the change in carrier density due to sputter deposition occurs to a depth much deeper than the

depletion region probed, because unlike thermal deposition techniques, in plasma sputtering, the ions in the plasma gain significant energy before colliding with the substrate. Therefore, at the time of arrival, these sputtered particles have energies many times larger than the binding energy of the surface of the substrate and therefore can penetrate deeper into the material. It is therefore clear that sputter-related defects can diffuse a significant distance into the semiconductor [9].

The deviation from ideal thermionic emission as well as the reduction in the barrier height may be due to near-surface damage, changing the properties of the interface as well as deep level defects causing carrier generation and barrier height inhomogeneity, indicating poorer rectification due to sputter damage.

Fig. 2 depicts the DLTS spectra from sputter-induced defects and a control sample of *n*-GaAs, Si doped with concentration of 1.0×10^{15} cm^{-3} and 1.0×10^{16} cm^{-3}. The DLTS spectra were obtained at rate windows of 80 s^{-1} and in the 20–405 K temperature range by applying a reverse bias and filling pulse amplitude of −1 V and 1.4 V, respectively. For the control sample (curve (a)) we observed only the EL2 defect. For the sputtered diodes on 1.0×10^{16} cm^{-3} doped GaAs, we observed seven defects (S1, S2, S3, S4, S5 and S6a & S6b), as shown in curve (b). Curves (c) and (d) (recorded on 1.0×10^{15} cm^{-3} doped GaAs) indicate the S5 and S3 are metastable: By applying −2 V at 400 K for 10 min and cooling under the same bias, S5 transformed to S3 and when zero bias at 400 K was applied for 10 min, followed by cooling under the same bias, the S3 transformed back to S5. Similarly, the S1 defect was metastable, and, as seen in Fig. 2, applying a reverse bias of −2 V at 400 K for 10 minutes introduced the S1 while zero bias at 400 K for 10 minutes totally removed it. However, no new defects was observed when the S1 was removed.

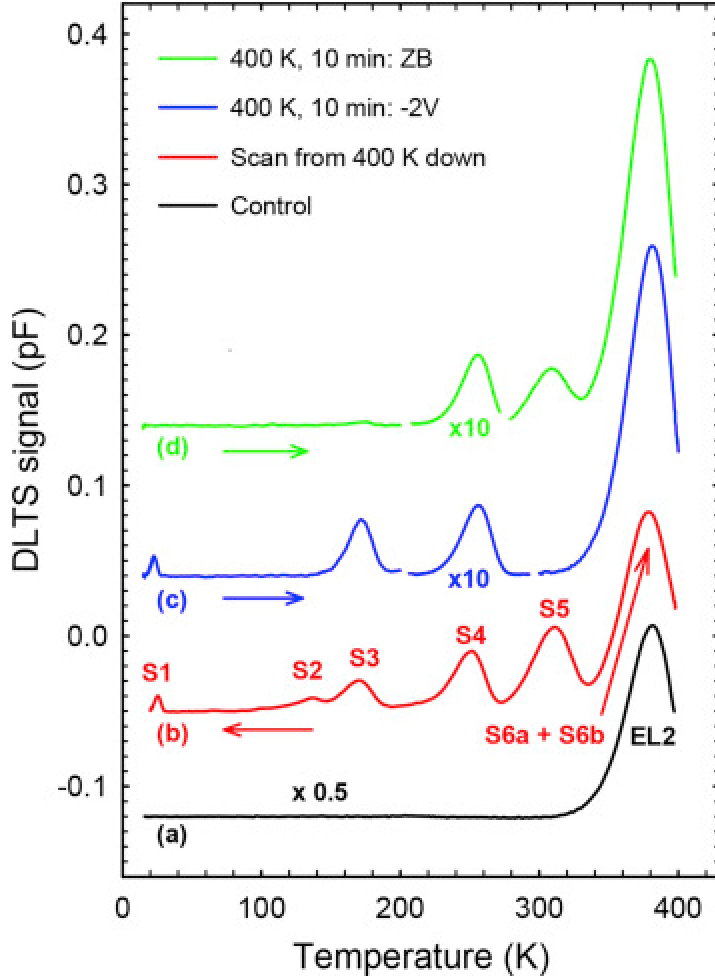

Fig. 2. DLTS spectra of (a) a control sample, (b) sample (1.0×10^{16} cm^{-3} Si doped) directly after sputtering, (c) sputtered sample (1.0×10^{15} cm^{-3} Si doped) after applying −2 V at 400 K for 10 minutes and (d) sputtered sample (1.0×10^{15} cm^{-3} Si doped) after applying zero bias for 10 minutes at 400 K. The reverse bias, V_r, and filling pulse amplitude, V_p, were −1.0 and 1.4 V, respectively with 1 ms pulse width and the rate window was 80 s^{-1} for all samples.

From Fig. 2 it is also clear that the S4 defect was highly dependent on the carrier density and the peak height decreased by about a factor ten when the dopant concentration was reduced by a factor 10. Note that in curves (c) and (d) the S4 peak height was multiplied by a factor of 10. The S2 was only observed in one of the 1.0×10^{16} cm^{-3} doped samples, the reason for this is not yet clear.

Fig. 3 shows Arrhenius plots of the seven sputter-induced defects (at 26 K, 140 K, 180 K, 265 K, 320 K and 384 K in Fig. 3) in n-type GaAs with a carrier concentration of 1.0×10^{15} cm^{-3}. The activation energies of the sputter-induced defects are listed in Table 2. As seen in Fig. 3 the activation energy and apparent capture cross-sections of the sputter-induced defects differed from those of the high energy electron irradiation-induced defects. Laplace DLTS measurements (see later) showed that the S6 defect had two components which we labelled S6a and S6b. Some of the sputter-deposition induced defects were similar to sputter-etching induced defects reported by Venter et al. [10], nitride encapsulation [11] and hydrogen plasma treatment [12,13] (Comparison included in Table 2).

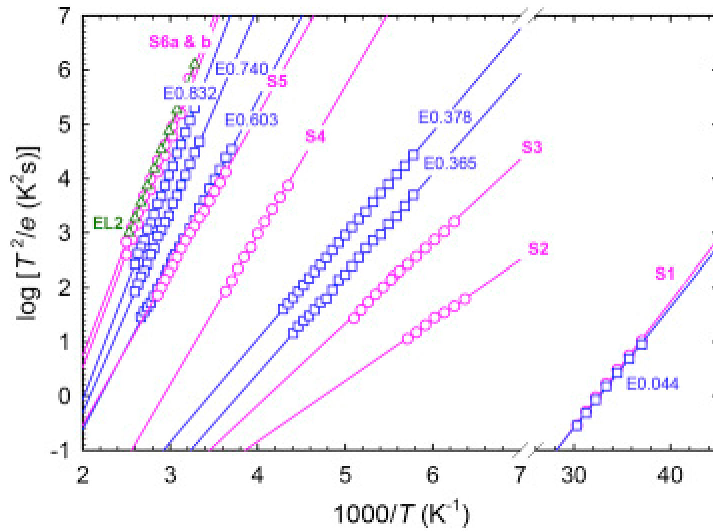

Fig. 3. Arrhenius plots of sputter-deposition induced defects (circle symbols), *n*-GaAs electron irradiation-induced defects (square symbols, labelled as in Table 1) and the EL2 (triangle symbols).

Table 2
Electronic properties of sputter-induced defects (S1–S6), Stress related or nitride capping induced defects [11], hydrogen plasma induced defect [12,13], Ar plasma-etching induced defects [9], electron-irradiation induced defects and the EL2.

Defect label	Origin[a]	E_A (eV)	σ_a (cm^2)	Stability
S1	S	0.046	3.1×10^{-13}	Metastable
E1' [9]	P	0.040	5.3×10^{-14}	Metastable
S2	S	0.22	1.9×10^{-15}	Stable
S3	S	0.30	1.6×10^{-14}	Metastable (transformed to S5)
M4 [11]	NC	0.31	1.8×10^{-18}	Metastable (transformed to M3)
M4 [13]	H	0.30	–	Metastable (transformed to M3)
M4 [12]	H	0.30	–	Metastable (transformed to M3)
E(0.31) [9]	P	0.31	5.2×10^{-14}	Metastable (transformed to E0.61)
S4	S	0.55	1.0×10^{-12}	Stable
S5	S	0.56	1.3×10^{-14}	Metastable (transformed to S3)
M3 [11]	NC	0.61	5.1×10^{-18}	Metastable (transformed to M4)
M4 [13]	H	0.50	–	Metastable (transformed to M4)
M3 [12]	H	0.55	–	Metastable (transformed to M4)
E(0.61) [9]	P	0.61	7.1×10^{-14}	Metastable (transformed to E0.31)
S6a	S	0.83	8.8×10^{-13}	Stable
S6b	S	0.84	6.6×10^{-13}	Stable
E(0.044)	E	0.044	1.9×10^{-14}	Stable
E(0.365)	E	0.365	8.7×10^{-14}	Stable
E(0.378)	E	0.378	3.6×10^{-14}	Stable
E(0.603)	E	0.603	4.9×10^{-14}	Stable
E(0.740)	E	0.740	5.7×10^{-14}	Stable
E(0.832)	E	0.832	2.8×10^{-12}	Stable
EL2	N	0.82	3.2×10^{-13}	Stable

[a] S = Sputter (current study), NC = Stress related or/Nitride capping [11], H = Hydrogen plasma [12,13], P = Plasma etched (Ar) [10], E = electron irradiation and N = Native defect.

Fig. 4 depicts the Laplace DLTS results for the S6 defect in the sputtered sample and the EL2 defect in the control sample. It is clear that the S6 defect has two components (S6a and S6b) and they do not directly correspond to the EL2 defect. It is interesting that the EL2 defect in the control sample had a small component that was not previously observed. The samples that were sputter deposited did not have the EL2 defect, and we speculate that the EL2 was modified to S6a and S6b.

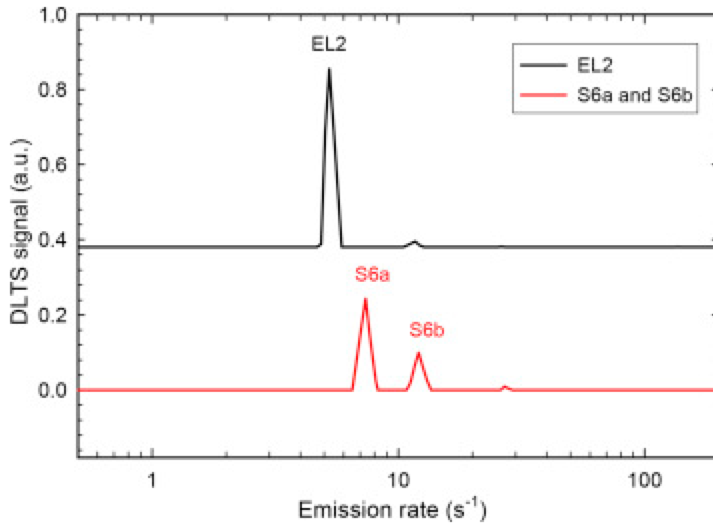

Fig. 4. Laplace spectra of EL2 and S6 defects as observed in 1.0×10^{15} cm^{-3} doped material. Both spectra were recorded at 350 K with a reverse bias of −1 V and a filling pulse amplitude of 1.4 V.

As shown in Fig. 3, the S3 and S5 defects were metastable. From Fig. 5, it is evident that the S3 transformed into the S5 after annealing under zero bias at 400 K for 10 minutes followed by cooling down under zero bias to 295 K, where the spectrum was measured under a bias of −1 V. Similarly, S5 could be transformed back to S3 under reverse bias (−2 V) while annealing at 400 K for 10 minutes followed by cooling down under −2 V to 180 K where the spectrum was measured under a bias of −1 V. It is interesting to observe the direct correlation between the concentration of S3 and S5. Fig. 5 shows the introduction and removal curves of the metastable defects. Transformation curves were measured by transforming as much as possible of the defect into one state at 400 K (−2 V bias for the S3, 0 V bias for the S5) followed by cooling (under the same bias conditions) to the annealing temperature, where the sample was annealed under the transformation conditions (0 V bias or −2 V bias respectively) for 5 minutes, followed by rapid cooling to the measurement temperature (295 K or 180 K) under the transformation conditions.

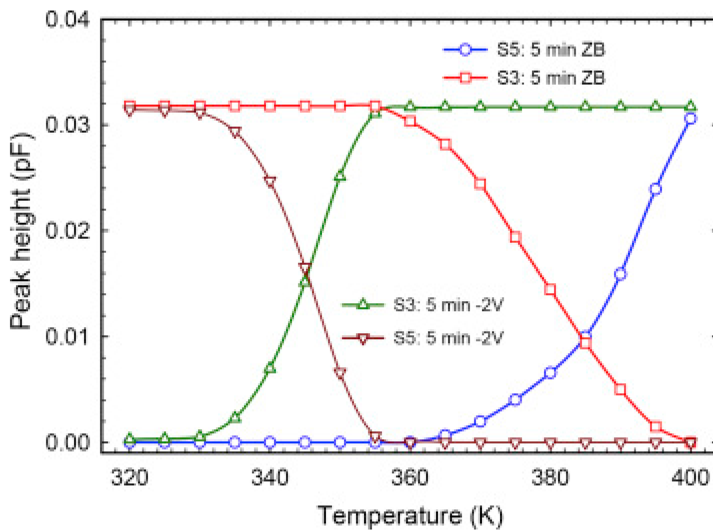

Fig. 5. Introduction and removal of S3 and S5 metastable defects. The conditions for the transformations are indicated in the figure.

The isochronal transformation of S3 → S5 and S5 S3 was modelled by first order kinetics:

$$N_X(t, T) = N_0[1 - \exp(-te_o(T))] \quad (1)$$

and

$$N_Y(t,T) = N_0\exp[-te_0(T)] \quad (2)$$

where N_X corresponds to the defect being removed and N_Y to the defect being introduced.

In these equations, N_0 is the maximum defect concentration, t is the annealing time in seconds and $e_0(T)$ is the temperature dependent transformation rate, in s^{-1}. The transformation rates can be written as:

$$e_0(T) = \alpha \exp(-E/kT) \quad (3)$$

In this equation, α, is a pre-factor with units of s^{-1}, E is the activation barrier for the particular transformation of the defect and k is the Boltzmann constant.

In Fig. 6, Arrhenius data of introduction and removal rate of S3 and S5 metastable defects are shown and transformation rate for each one was calculated.

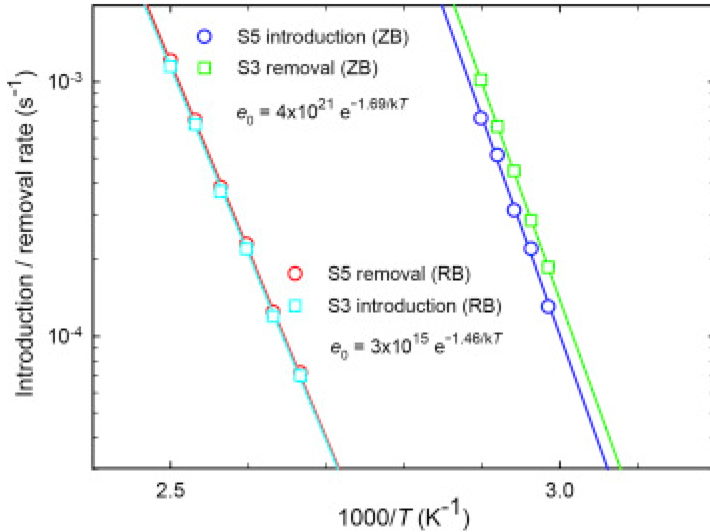

Fig. 6. Arrhenius data for the transformation of S3 → S5 and S5 → S3.

In these transformation rates we have 3×10^{15} s^{-1} and 4×10^{21} s^{-1}, respectively, as pre-factors for equation. (3). The pre-factor obtained from our measurements to transform S5 from S3 is almost the same as the one reported by Buchwald et al. [11] (10^{21} s^{-1} pre-factor of formation M4 and decay of M3). For the transformation of S3 to S5 the pre-factor was 10^{15} s^{-1}, which is higher than the 10^7 s^{-1} reported by Buchwald et al. [11], 10^8 s^{-1} reported by Conibear et al. [12] and 10^{11} s^{-1} reported by Pfeiffer and Weber [13].

The pre-factor α can be physically related to the attempt frequency of the process and can be used to deduce the physical mechanism leading to the temperature dependence. Some mechanisms identified so far [14] include elementary atomic jump ($\alpha \sim 10^{12}$ s^{-1}), free-carrier

capture by multiphonon emission ($\alpha \sim 10^7$ s^{-1}), free-carrier emission ($\alpha \sim 10^{13}$ - 10^{14} s^{-1}). The high prefactor for the transformation of S3 to S5 ($\alpha \sim 10^{21}$ s^{-1}) is even larger than would be expected for direct free-carrier capture by a potential well with a large capture cross-section. The smaller capture prefactor for the transformation S5 to S3 seems to indicate free carrier emission.

4. Conclusions

Au Schottky barrier contacts (SBDs) were fabricated on n-type GaAs using DC sputtering and their electrical properties were investigated. *I-V* and *C-V* results indicate that the ideality factor and Schottky barrier height significantly changed compared to the resistively deposited control sample. DLTS spectra were recorded over a temperature range of 20–400 K. Sputter deposition introduced seven defects in GaAs, of which the energy levels range from E_c – 0.046 eV to E_c – 0.84 eV, of which one was highly dopant dependent. Laplace DLTS was used to characterize the defects. From the Arrhenius plots we extracted the activation energy and apparent capture cross-section of each defect. One defect, labelled the S6, consisted of two different components and differed significantly from the EL2 defect which appears in the same temperature range, but was not observed in the sputtered samples.

None of the defects were similar to those observed after electron irradiation but three were similar to those found in nitride encapsulation, hydrogen plasma and Ar plasma etched samples. Annealing the sample at 400 K under two different bias conditions, namely -2 V and 0 V, showed that three of them are metastable. Two peaks, E_c – 0.30 eV and E_c – 0.56 eV, transformed into each other with electron capture being the rate determining step for one of the transformation processes. The E_c – 0.046 eV defect was metastable as well but we could not find the defect which it transforms into.

Acknowledgements

This work is based on the research supported by the National Research Foundation of South Africa under grant number 98961. Opinions, findings and conclusions or recommendations are that of the authors, and the NRF accepts no liability whatsoever in this regard. The Laplace DLTS software and hardware used here was received from L. Dobaczewski (Institute of Physics, Polish Academy of Science) and A. R. Peaker (Center for Electronic Materials Devices and Nano-structures, University of Manchester).

References

[1] F.D. Auret, O. Paz, N.A. Bojarczuk, Characterization of process-induced defects and device properties of ion beam sputter-deposited Mo contacts on Si, J. Appl. Phys. 55 (6) (Mar. 1984) 1581–1589.
[2] Y. Leclerc, F.D. Auret, S.A. Goodman, G. Myburg, C. Schutte, Electronic properties of defects introduced during sputter deposition of Cr Schottky contacts on GaAs, Ion Beam Modification of Materials, Elsevier, 1996, pp. 870–873.
[3] F.D. Auret, S.A. Goodman, G. Myburg, W.O. Barnard, Electrical characterization of sputter-deposition-induced defects in epitaxially grown n-GaAs layers, Vacuum 46 (8–10) (Aug. 1995) 1087–1090.
[4] F.D. Auret, S.A. Goodman, G. Myburg, W.E. Meyer, Electrical characteristics of Arion sputter induced defects in epitaxially grown n-GaAs, J. Vac. Sci. Technol. B Microelectron. Nanom. Struct. 10 (6) (Nov. 1992) 2366.

[5] D.A. Vandenbroucke, R.L. Van Meirhaeghe, W.H. Laflere, F. Cardon, "Sputter-induced damage in Al/n-GaAs and Al/p-GaAs Schottky barriers," *Semicond*, Sci. Technol. 2 (5) (May 1987) 293–298.
[6] W.J. Devlin, R.F. sputtered Au-Mo contacts to n-GaAs, Electron. Lett. 16 (3) (1980) 92.
[7] M.G. Lupo, A. Cola, L. Vasanelli, A. Valentini, Deep level transient spectroscopy of Mo/GaAs Schottky barriers prepared by DC sputtering, Phys. Status Solidi 124 (2) (Apr. 1991) 473–481.
[8] L. Dobaczewski, A.R. Peaker, K. Bonde Nielsen, Laplace-transform deep-level spectroscopy: the technique and its applications to the study of point defects in semiconductors, J. Appl. Phys. 96 (9) (2004) 4689–4728.
[9] A.H. Eltoukhy, J.E. Greene, "Diffusion enhancement due to low-energy ion bombardment during sputter etching and deposition, J. Appl. Phys. 51 (8) (Aug. 1980) 4444–4452.
[10] A. Venter, et al., Ar plasma induced deep levels in epitaxial *n* -GaAs, J. Appl. Phys. 111 (1) (Jan. 2012) 013703.
[11] W.R. Buchwald, G.J. Gerardi, E.H. Poindexter, N.M. Johnson, H.G. Grimmeiss, D.J. Keeble, Electrical and optical characterization of metastable deep-level defects in GaAs, Phys. Rev. B 40 (5) (Aug. 1989) 2940–2945.
[12] A.B. Conibear, A.W.R. Leitch, C.A.B. Ball, Third metastable hydrogen-related level in n -type GaAs, Phys. Rev. B 47 (4) (Jan. 1993) 1846–1848.
[13] G. Pfeiffer, J. Weber, Metastable defects in N-type GaAs related to hydrogen, Mater. Sci. Forum 143–147 (Oct. 1993) 873–878.
[14] A. Chantre, Introduction to defect bistability, Appl. Phys. Solid Surf. 48 (1) (Jan. 1989) 3–9.